RSC Advances

This is an *Accepted Manuscript*, which has been through the Royal Society of Chemistry peer review process and has been accepted for publication.

Accepted Manuscripts are published online shortly after acceptance, before technical editing, formatting and proof reading. Using this free service, authors can make their results available to the community, in citable form, before we publish the edited article. This *Accepted Manuscript* will be replaced by the edited, formatted and paginated article as soon as this is available.

You can find more information about *Accepted Manuscripts* in the **Information for Authors**.

Please note that technical editing may introduce minor changes to the text and/or graphics, which may alter content. The journal's standard **Terms & Conditions** and the **Ethical guidelines** still apply. In no event shall the Royal Society of Chemistry be held responsible for any errors or omissions in this *Accepted Manuscript* or any consequences arising from the use of any information it contains.

www.rsc.org/advances

RSC Advances

ARTICLE

Versatile bi-metallic Copper-Cobalt catalyst for liquid phase hydrogenation of furfural to 2-methylfuran

Sanjay Srivastava, G. C. Jadeja, Jigisha Parikh[*]

Liquid phase hydrogenation of furfural (FFR) to 2-methyl furan (2-MF) was examined using noble metal free, Cr-free, bi-metallic Cu-Co catalysts. Three supported bi-metallic catalysts (Cu-Co/SiO$_2$, , Cu-Co/H-ZSM-5, and Cu-Co/ɣ-Al$_2$O$_3$) with various Cu/Co molar ratios (x/y=1, 2, and 4) with fixed Cu loading (x=10 wt%) were prepared by the impregnation method. The physico-chemical properties of various catalysts were studied by using XRD, N$_2$-sorption, SEM, TEM, TPR, TPD, XANES/EXAFS and CHNS methods. The results confirmed the formation of spinel CuCo$_2$O$_4$ oxides, and much higher dispersion of Cu on acidic supports such as H-ZSM-5 and ɣ-Al$_2$O$_3$. However, absence of spinel CuCo$_2$O$_4$ oxide was observed in Cu-Co/SiO$_2$ via XANES/EXAFS results. XRD and TEM results revealed the formation of bigger Cu particles in Cu-Co/SiO$_2$. In the catalytic acitivity studies, Cu-Co/ɣ-Al$_2$O$_3$ catalyzed the hydrogenation of furfural with 98.8% conversion, resulting in maximal selectivity of 2-MF due to the presence of maximal Cu-CoOx sites. H-ZSM-5 supported catalyst had marginally less 2-MF selectivity, whereas silica supported catalyst exhibited maximum selectivity towards furfuryl alcohol (FOL) because of the large copper particles. H$_2$-TPR and EXAFS results revealed that the incorporation of cobalt metal improves the reducibility of Cu-catalysts, thus improving the catalytic activity. Bi-metallic Cu-Co/ɣ-Al$_2$O$_3$ catalysts displayed higher activity as compared to their monometallic counterpart, and Cu-Co/ɣ-Al$_2$O$_3$ (x/y=1) exhibited the best catalytic performance with 78% selectivity to 2-MF at 220 ^{o}C and 4 MPa.

Introduction

Nowadays, 85% of the world's energy demands rely on fossils derived energy and fuels.[1] Due to the ultimate diminution of crude oil reserves together with increasing anthropogenic emissions of greenhouse gases, climate change, and ever increasing prices of petroleum crude, search for renewable resources has attracted worldwide attention leading to the development of new energy alternatives for the possible substitution of fossil reserves.[2,3] The conversion of lignocellulosic biomass (only carbon containing renewable feedstock) into bio-oil is of special interest because of its wide availability.[4] However, direct use of bio-oil is restricted as a fuel due to its adverse properties such as low calorific value, deficient volatility, acidity, and instability, which were not compatible to the I. C. engine.[5] The undesirable properties of bio-oil are attributed to the presence of different class of oxygenates such as aldehydes, acids, and ketones. These oxygenates often condense and polymerize during storage owing to their high reactivity.[5, 6] The removal of oxygen is thus mandatory to convert bio-oil into a liquid fuel. [7]

Furfural (FFR) is one of the innumerable oxygenated compounds which is found in bio-oil, containing both C=C and C=O bonds. The C=C stays within one 5 member ring and 6 electrons stabilized

system that makes the C=C bond very stable.[8,9] Therefore, hydrogenation of C=O bond was often catalyzed, resulting in furfuryl alcohol (FOL) as a primary product, and further hydrogenolysis of FOL enables 2-methyl furan (2-MF) (see Scheme.1). As compared with hydrocarbons, 2-MF contains the oxygen atom having better combustion performance and the higher research octane number (RON=103) than that of gasoline (RON=96.8).[10] Owing to this admirable property, 2-methyl furan has been recently used as a gasoline blend in standard vehicles.[11] In other applications, 2-MF is used as perfume intermediates, chloroquine lateral chains in medical intermediates, and as a raw material for the production of crysanthemate pesticides.[11,12]
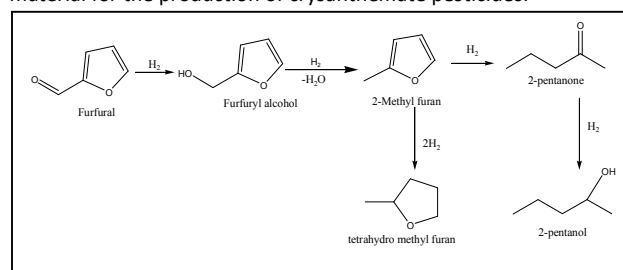
Scheme.1 Hydrogenation of furfural to 2-methylfuran

Hydrogenation of furfural to 2-methylfuran can take place both in the vapour and in the liquid phase due to its high vapour pressure.[13] The vapour phase conversion of FFR to 2-MF has been widely studied over Raney-Cu, Cu/SiO$_2$, Cu/SBA-15, Cu/MgO, Cu-Mn-Si, Cu-Zn-Al, Ni-Fe/SiO$_2$ at a high temperature range (250-270°C).[13-19] However, deactivation of supported Cu-catalysts is a key issue in vapour phase hydrogenation, although they could be regenerated

Department of Chemical Engineering, Sardar Vallabhbhai National Institute of Technology, Surat-395007, Gujarat, India

via calcinations above 500°C.[12] In addition, vapour phase hydrogenation of furfural produces not only the 2-MF but also a wide range of by products, including furan, tetrahydrofuran (THF), and even C-4 products.[18]

In contrast, liquid phase hydrogenation is most likely preferred for compatibility with the upstream production of furfural.[13] The liquid phase hydrogenation of furfural to 2-methyl furan has been performed either on noble metals such as Ru, and Pt [13, 20-22] or Cu-Cr, and Cu-Fe catalysts.[10-12] Yan et al. [10, 11] have reported the liquid phase synthesis of 2-MF via furfural using Cu-Cr, and Cu-Fe catalysts, wherein a reasonable yield of 51% was reported over a Cu-Fe catalyst at 220°C and 90 bar. However, such high temperature and pressure can account for the extra energy cost. In addition, owing to high toxicity and environmental concern for Cu-Cr alloys, its use has been restricted as industrial catalyst.[11,23] Recently, Paraskevi et al.[13] have reported the moderate yield of 2-MF (61%) over a Ru/C catalyst at temperature of 220°C. The research done so far in this area manifests the incompatibility of most of the catalysts for industrial applications owing to certain disadvantages, such as severe environmental concerns, the low selectivity, the high cost, and ruthless deactivation. Thus, an efficient, cost effective, environmentally benign and a stable catalyst for FFR hydrogenation to 2-MF is the need of the hour. Recently, a highly stable bimetallic Cu-Co catalyst has shown good versatility as it can be used in many reactions including FT-synthesis and other hydrogenation reactions.[24-28] The major advantage of this bi-metallic catalyst system is the presence of metallic copper and partially reduced cobalt species.[29-32] Furthermore, the strong interaction between copper and cobalt may result in the formation of mixed oxide phases.[33] Xu et al.[34] have reported that early transition metal oxides such as CoOx, ReOx, and MnOx etc., can break the C-O bond. Therefore, the combination of Cu metal and CoOx can be effective in the production of 2-MF via hydrogenation/hydrogenolysis process using bi-metallic Cu-Co system. In our previous work, we have reported the higher conversion of furfural to furfuryl alcohol over SBA-15 supported Cu-Co catalysts.[27-28]

Consequently, in the present study noble metal free, and Cr-free bi-metallic Cu-Co catalysts with various Cu/Co molar ratios (x/y=1, 2, and 4) over different supports such as SiO_2, H-ZSM-5, and γ-Al_2O_3 were prepared. Further, the ability of synthesized catalysts was explored towards production of 2-MF via liquid phase hydrogenation of FFR. Subsequently, the effect of temperature (140-220 °C) was studied over Cu-Co/γ-Al_2O_3 (x/y=1).

Experimental

Material

Metal precursors such as cobalt nitrate (Co $(NO_3)_2.6H_2O$), copper nitrate (Cu $(NO_3)_2.6H_2O$); Chemicals such as furfural, furfuryl alcohol, 2-methyl furan, 2-methyltetrahydrofuran, 2-pentanone, and 2-pentanol (all GC grade) were purchased from Sigma-Aldrich, Mumbai, India. Supports such as SiO_2, H-ZSM-5 (Si/Al=25), and γ-Al_2O_3 having purity (99%) were purchased from the local vendor.

Catalysts synthesis and characterization

The bi-metallic Cu-Co catalysts with various Cu/Co molar ratios (x/y=1, 2, and 4) over different supports such as SiO_2, H-ZSM-5, and γ-Al_2O_3 were synthesized by impregnation method using salt of respective metals. The prepared catalysts were characterized by X-ray diffraction (XRD), N_2- adsorption desorption, field emission-scanning electron microscopy analysis (FE-SEM), transmission electron microscopy analysis (TEM), ammonia-temperature-

programmed desorption(NH_3-TPD), H_2-temperature programmed reduction (TPR), X-ray absorption spectroscopy (XANES)/(EXAFS), and CHNS elemental analysis. The detailed procedures regarding the synthesis and characterization of catalysts are provided in the supplementary information.

Catalytic activity study

Catalytic activity studies were performed in a 100 mL autoclave reactor using 2-propanol as a solvent. Briefly, in a typical experiment, 1 g of catalyst was reduced at 280±2°C by passing H_2 at pressure of 1 MPa for 3 h. The reactor was then cooled down to room temperature and flushed with N_2. Furfural (3.72 mL) was initially added into 2-propanol solvent (20 mL) and charged into the reactor. The catalytic activity of prepared catalysts was investigated at 140-220°C under hydrogen pressure of 4 MPa with stirring speed at 1000 rpm, thereby ensuring the absence of gas-liquid, liquid-solid, and intra-particle mass transfer limitations.[35] The reproducibility of the experimental analysis was ensured by repeating each run twice; the reproducibility was within acceptable limits. Product samples were analysed using a Sigma GC system with FID detector. The Carbowax capillary column with dimension of 30 m x 0.25 mm x 0.5μm was used. In a typical procedure, the initial oven temperature was held at 80°C for 4 min and increased up to 220 °C with the ramp of 20 °C/min and hold for 4 min. The product suspension (1μL) in 2-propanol was injected into the capillary column by using the split ratio of 20:1, where nitrogen was used as a carrier gas. The catalytic parameters such as conversion, and selectivity were calculated by using the following formulae:

$$C(\%) = \frac{Xinitial - Xfinal}{Xinitial} X\ 100 \ . \ (i)$$

$$S(\%) = \frac{moles\ of\ desired\ product\ formed}{total\ moles\ of\ all\ products\ formed} X\ 100 \ …\ …\ (ii)$$

(C= FFR conversion, S= Selectivity, X= FFR moles)

Result and discussion

Catalysts characterization

Figure.1 shows XRD spectra of bi-metallic Cu-Co (x/y=1) catalysts supported on SiO_2, H-ZSM-5, and γ-Al_2O_3. As observed, the bimetallic catalysts contain either segregated CuO, or spinel oxides of Co_3O_4/$CuCo_2O_4$. Owing to a similar cubic framework and approximately similar unit cell parameters (aCo_3O_4 = 8.177 and a$CuCo_2O_4$ = 8.122 A), Co_3O_4 and $CuCo_2O_4$ were not easily distinguishable from their XRD patterns[33], which were further confirmed using XANES/EXAFS analysis. Cu-Co/ SiO_2 (x/y=1) catalyst showed sharp diffraction patterns at 2θ = 35.5°, 38.7° which are assigned to the planes (111) and (111) of monoclinic copper oxide (JCPDS, 80-1917, 45-0937),[16,26,36] and few diffraction patterns pertaining to the Co_3O_4 at 2θ = 37°, 44°, and 56° (JCPDS, 43-1003).[26,33,37] Sharp diffraction peaks indicate the presence of large metallic crystallite sizes in Cu-Co/SiO_2. In SiO_2 supported catalyst, the size of the CuO crystallite was found to be in the range of 35 to 40 nm, as calculated by the Scherrer formula. On the other hand, Cu-Co (x/y=1) catalysts supported on acidic carriers, i.e. H-ZSM-5 and γ-Al_2O_3, showed mixed reflections of CuO, Co_3O_4, and spinel oxides of Co_3O_4/$CuCo_2O_4$.[26,33]

The smaller size metal particles were found in the case of both H-ZSM-5 and γ-Al_2O_3 supported catalysts. The size of metal particles lies in the range of 15-20 nm as calculated by the Scherrer formula. These observations are in well accordance with those previously reported.[31,32] The difference in the phases obtained with different

supports may be explained on the basis of a distinct metal –metal and metal-support interactions. It is worth noting that all the oxide supports used in the present study have weak interaction with copper and cobalt[38], and the pattern of interaction follows as SiO_2 > H-ZSM-5> γ-Al_2O_3. In addition, both copper and cobalt metals are known to possess strong interaction between them[33]. Accordingly, the relatively stronger interaction of copper and cobalt with SiO_2 resulted in segregated phases of CuO and Co_3O_4, having bigger sizes, whereas the weaker interaction of copper and cobalt oxides with acidic supports resulted in the formation of $CuCo_2O_4$ phase. These observations are well matched with previous reports,[33] wherein the presence of bi-metallic Cu-Co phases were confirmed at even low Cu content (5%). Figure.1S depicts the XRD patterns of Cu-Co/γ-Al_2O_3 with various Cu/Co ratios (x/y= 1, 2, and 4). An increase in the intensity of the peaks was observed when Cu/Co ratio decreased from 4 to 1. This increase in intensity is due to an agglomeration of the metal particles which was further justified by the BET surface area and SEM micrographs. In addition, few peaks pertaining to the Co_3O_4 appeared with an increase in Co metal which suggests the preferential localization of cobalt oxide particles in alumina pores, attributed to the high loading of Co.[33,37]
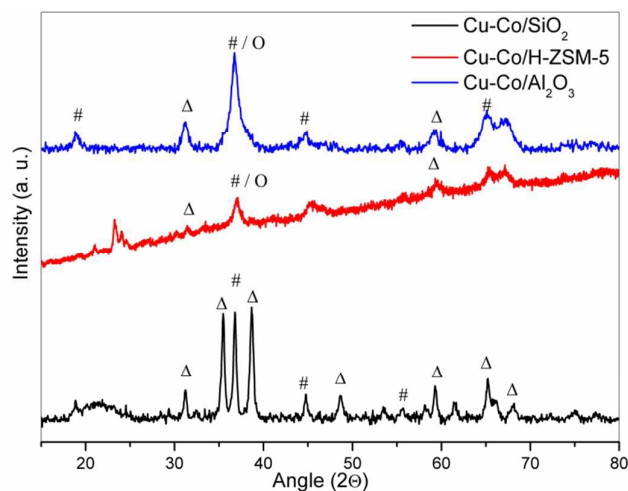
Figure.1 XRD patterns for supported Cu-Co (x/y=1) catalysts [(o) $CuCoO_4$, (#) Co_3O_4 (Δ) CuO]

The textural properties of supports and synthesized catalysts Cu-Co (x/y=1) over different supports such as SiO_2, H-ZSM-5, and γ-Al_2O_3 are summarized in Table.1 It was observed that silica supported catalyst shows the large decrease in the % surface area of parent material as compared to acidic supports H-ZSM-5 and γ-Al_2O_3. Decline in the surface area can be attributed to the nature of supports as silica had a stronger interaction with both metals used in the present work. [30]

Table 1. Textural and structural characteristics of various supports

Catalysts/ Supports	Cu/Co molar ratio (x/y)	EDX (x:y) wt%	Surface area (m²/g)	Pore volume (cm³/g)	Pore size (Å)	Avg. Particle Size (nm)
SiO_2			179.4	0.34	42	
H-ZSM-5			392.5	0.46	64	
γ-Al_2O_3			166.1	0.54	66	
Cu-Co/ SiO_2	1	9.2:8.4	102.6	0.17	28	35
Cu-Co/ H-ZSM-5	1	10.6 :10.2	239.9	0.34	58	15
Cu-Co/ γ-Al_2O_3	1	10.4 :9.9	113.5	0.32	46	20

Effects of Cu/Co ratios on textural and structural characteristics of Cu-Co/ γ-Al_2O_3 are presented in Table S1. The gradual decrease in surface area, pore volume, and pore size were observed with decreasing Cu/Co ratio. This may be attributed to the agglomeration of metal particles within the pores of γ-Al_2O_3 due to high loading of metal particles.

The morphology of Cu-Co (x/y=1) catalysts in the bulk and on surface of SiO_2, H-ZSM-5, and γ-Al_2O_3, are presented in Figure 2. The distinct morphology of all the three catalysts appeared with a little agglomeration of metal particles over different supports. Uniform distribution having small metal crystallites was observed in Cu-Co/γ-Al_2O_3 (x/y=1). Similar dispersion having large metal crystallites was observed in Cu-Co/ SiO_2 (x/y=1). However, non-uniform distribution having un-even sizes of metal crystallites appeared in Cu-Co/H-ZSM-5. The shape and the size of the fresh Cu-Co/ γ-Al_2O_3 (x/y=1, 2, and 4) catalysts are presented in Figure S3. An average crystallites size was increased with increasing doping of the second metal (Co) as revealed by SEM data. The size of crystallites in Cu-Co/ γ-Al_2O_3 (x/y=4) lies between 10-15 μm, in Cu-Co/γ-Al_2O_3 (x/y =2) lies between 20-25 μm, and in Cu-Co/γ-Al_2O_3 (x/y =1), it lies between 20-30 μm. Furthermore, samples were examined using energy dispersive X-ray microanalysis (EDX) to quantify the metal loadings (in wt. %) and the results were compared with actual metal loadings deposited during the preparation (refer. Table 1 & Table S1). As compared with the actual metal loadings of the samples, EDX results are well supported within the limit of acceptable error.
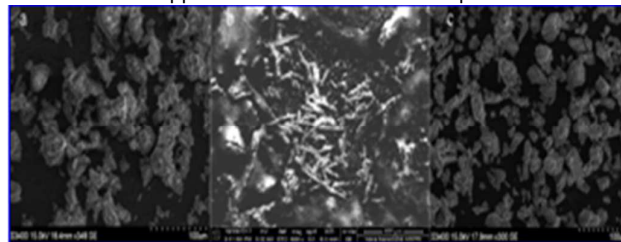
Figure 2. Scanning electron micrographs of Cu-Co (x/y =1) over (a) SiO_2, (b) H-ZSM-5, (c) γ-Al_2O_3,
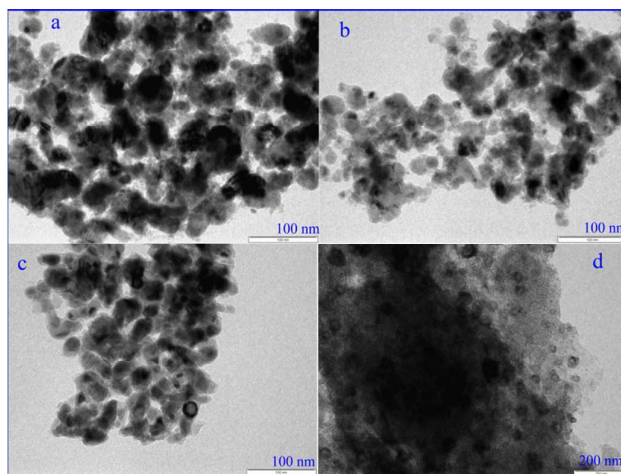
Figure 3. Transmission electron micrographs of Cu-Co (x/y =1) over (a) SiO_2, (b) H-ZSM-5, (c) γ-Al_2O_3, (d) used Cu-Co (x/y =1)/γ-Al_2O_3 (2nd cycle)

The TEM micrographs of freshly reduced Cu-Co (x/y =1) over different supports, and used Cu-Co (x/y =1)/γ-Al₂O₃ (2ⁿᵈ cycle) without calcinations are presented in Figure.3. As observed, metal-support interaction plays key role in stabilizing the morphology/ordering of the Cu-Co nanoparticles. Ordered large metal nanoparticles were observed in SiO₂ supported catalysts owing to stronger metal-support interaction between silica and metal particles. However, over H-ZSM-5, the Cu-Co nanoparticles were found to be non-uniformly distributed. Whereas, Cu-Co/γ-Al₂O₃ showed well dispersed and ordered small nanoparticles having uniform spherical shape as evident from the pictorial view. Furthermore, the size of copper-cobalt nano-particles was different to a certain extent, as Cu-Co/H-ZSM-5 contains mixed sizes of particles (15-25 nm). However, Cu-Co/ γ-Al₂O₃ showed mostly uniform size about 20 nm. This morphology/ordering of the Cu-Co nanoparticles over both H-ZSM-5 and γ-Al₂O₃ catalysts can be explained on the basis of a combination of porous structure and metal-support interaction. The more uniform distributions of copper-cobalt particles over γ-Al₂O₃ support may be ascribed to weaker interaction of uniform porous alumina to both copper-cobalt species amongst all three supports used. On the contrary, H-ZSM-5 has both Si and Al metals in it. So, there is a possibility of slightly stronger interaction, due to combined effect of Si and Al with copper and cobalt oxides. This may lead to deviation in the metal distribution on the catalyst support surface. Furthermore, there are different morphologies of Al in zeolites (such as tetragonal and octahedral). Hence, when these Al particles interact with copper and cobalt oxides, the particle size of copper and cobalt oxides may change to certain extent.[39]

The surface acidity of bi-metallic Cu-Co (x/y =1) catalysts supported on SiO₂, H-ZSM-5, and γ-Al₂O₃ was determined by NH₃-TPD experiments (Figure.4, Table. S2). Generally, the strength of acid sites which was determined by the NH₃ desorption temperature can be classified as weak (<250 °C), medium (250–400 °C) and strong (>400 °C) acidic sites. The overall acidity in various catalysts can be calculated from the relative peak area of NH₃-desorption curves.[37] As expected, reduced Cu-Co/SiO₂ (x/y =1) showed insufficient weak acid sites, as SiO₂ had scarcely the acidic property. Cu-Co/γ-Al₂O₃ (x/y =1) showed three peaks (145 °C, 335 °C, and 555 °C) which can be ascribed to NH₃ desorption from weak, medium and strong acid sites. While, Cu-Co/H-ZSM-5 (x/y =1) showed two major peaks (<230-260> °C, and <400-450> °C) which can be ascribed to NH₃ desorption due to the presence of medium and strong acid sites (refer. Figure.3, and Table S2). It was observed that an acidity of both γ-Al₂O₃ and H-ZSM-5 is improved (0.28 to 0.49 and 0.66 to 1.08) by the doping of Cu and Co. This may be attributed to the formation of CoOx and/or mixed Cu-Co phases over acidic supports.
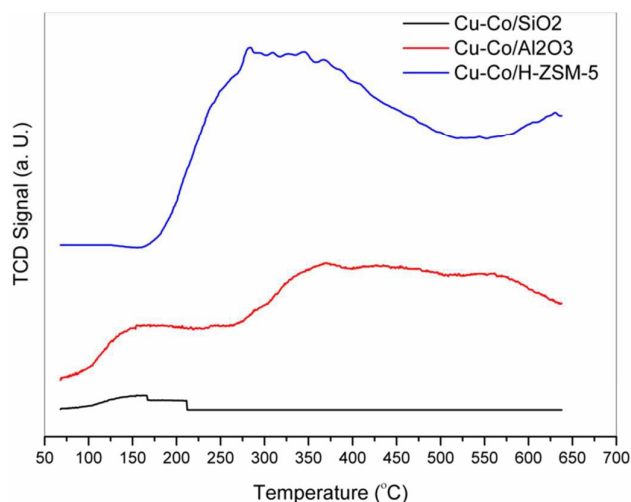
Figure 4. Ammonia-TPD profiles of Cu-Co (x/y =1) supported on SiO₂, H-ZSM-5, and γ-Al₂O₃

The surface acidity of Cu-Co/γ-Al₂O₃ (x/y =1, 2, and 4) catalysts changed with Cu/Co ratio (see. Figure. S4 and Table S3). However, total acidity was not at all influenced by the effect of Cu/Co ratio. It was observed that weak and moderate acid sites increased slightly with the decrease in a Cu/Co ratio (from 4 to 1), while for strong acidic sites, a reverse trend was observed and maximum strong acid sites were found at a Cu/Co (x/y =4) ratio. The strong acidic sites present in both the catalysts suggests the strong attraction of Cu to OH of alumina.[38] In addition, few copper species (after reduction) may be interacting with γ-Al₂O₃ owing to the high electron affinity of aluminium. This electron affinity of aluminium would seize electrons from metal copper. The transfer of electron density from metal copper to aluminium would increase the electropositive (or the oxophilic) nature of copper and the further improvement of the oxophilic nature would contribute to hydrogenolysis of the saturated C-O band.[32, 33]

To investigate the reducibility and structural evolutions of bi-metallic Cu-Co catalysts, H₂-TPR experiments were employed. Generally, when metal species interact with carriers by creating new surface compounds or altering their chemical states, their reduction temperature would change. Accordingly, the interaction of each metal component with supports would have significant influence on the chemical environment of metals. A weak interaction would favour the reduction of metal oxide to metal.[38] On the contrary, due to the presence of a strong interaction between metal species and supports, metal particles would face difficulty in getting reduced, and would result in low valence metal or incomplete reduction.[37, 38]

Figure.5 shows the reducibility of Cu-Co (x/y =1) catalysts supported on SiO₂, H-ZSM-5, and γ-Al₂O₃. It was observed that the nature of the support had a significant effect on the reducibility of bi-metallic catalysts. The differences in the reduction temperature revealed that SiO₂ (peak centred 305-345 °C) support had stronger interaction with both metals than γ-Al₂O₃ (peak centred 273 °C) and H-ZSM-5 (peak centred 242 °C). Cu-Co/SiO₂ (x/y=1) exhibited the highest reduction temperature as a result of the largest CuO crystallites and poor porous structure.
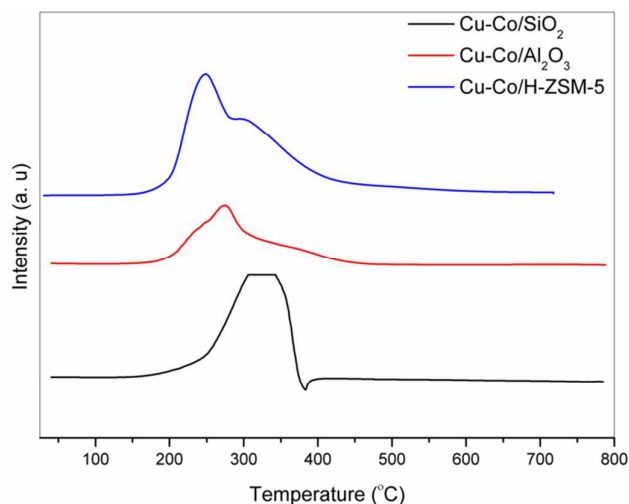
Figure 5. TPR pattern for Cu-Co (Cu/Co=1) supported on SiO_2, H-ZSM-5, and γ-Al_2O_3

Concomitantly, TPR patterns for other two catalysts (Cu-Co/ H-ZSM-5, and Cu-Co/ γ-Al_2O_3) were different and reduced at low temperature ascribed to the reduction of mixed copper-cobalt oxides and smaller copper particles. These observations were well supported by XRD, and TEM results. The occurrence of multiple reductions peaks indicated the two step reduction of copper, and partial reduction of $CuCo_2O_4$/Co_3O_4. The reduction of copper occurs in two steps such as $Cu^{2+} \rightarrow Cu^+$ at low temperature, and $Cu^+ \rightarrow Cu^o$ at high temperature [16, 35]. Furthermore, amongst all three supports, weaker interaction between alumina and copper-cobalt oxide phases enhances the reducibility of both the copper oxides and mixed $CuCo_2O_4$, and thus increasing Cu-CoOx sites in Cu-Co/γ-Al_2O_3.

Figure.6 displays the TPR patterns of bi-metallic Cu-Co/γ-Al_2O_3 catalysts with a various Cu/Co ratio (x/y= 1, 2, and 4), and comparison with their monometallic counterparts. The H_2-TPR profile of monometallic 10 wt% Co/ γ-Al_2O_3 displayed two hydrogen consumption peaks (at 504 and 657 ^{o}C). This can be attributed to the two - step reduction of Co_3O_4 to Co (0), which takes place via the intermediate CoO. [40, 41] The reduction of smaller CoO particles to Co (0) is often difficult and requires higher temperatures which can be attributed to the high-temperature broad TPR peak. The monometallic 10 wt% Cu/ γ-Al_2O_3 also showed two peaks (at 193 and 249 ^{o}C), which probably corresponds to the reduction of CuO; $Cu^{2+} \rightarrow Cu^+$ at low temperature, and $Cu^+ \rightarrow Cu^o$ at high temperature. In contrast, much different H_2-TPR patterns were observed for bimetallic Co-Cu/γ-Al_2O_3 catalysts with various Cu/Co ratio (x/y= 1, 2, and 4) due to strong interaction between Cu and Co species. It was believed that H_2–TPR proceeds through the reduction of both segregated (CuO) and mixed oxides. These observations are in good agreement with literature available for bimetallic Cu-Co catalysts. [31]

Furthermore, H_2-TPR profiles changed significantly with Cu/Co ratio. This behaviour of the catalysts may be attributed to the step wise reduction of Cu and its level of interaction with Co. In the Cu-Co (x/y=1), a broad peak was found with two lower shoulders appearing in between 321 to 354°C, whereas in case of Cu-Co (x/y=2), both the peaks started shifting to the slightly higher side. Cu-Co (x/y=4) revealed three distinct peaks, which might be due to

highly dispersed CuO at moderate temperature, and the formation of small Cu–Co clusters at higher temperature above 400 to 440 ^{o}C that can be observed distinctly(Figure.6).
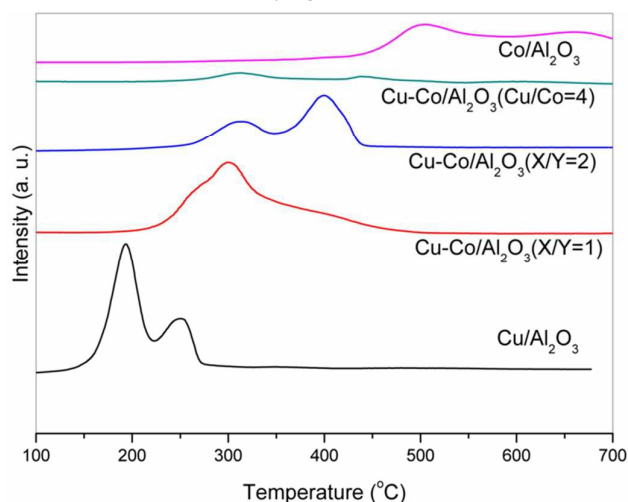
Figure 6. Comparison of H_2-TPR patterns of bi-metallic Cu-Co/γ-Al_2O_3 with various (Cu/Co) to monometallic Cu and Co supported on γ-Al_2O_3

XAS has provided extra information about copper and cobalt phases and their dispersion in prepared catalysts. The XANES and derivative XANES spectra of fresh calcined and reduced Cu-Co(X/Y=1) catalysts over various supports, and Cu-Co/ γ-Al_2O_3 (X/Y=1, 2, 4) were compared with Cu-foil, CuO references (Figure.7, S5). Copper oxide (Cu^{2+}) is likely to have the threshold binding at higher energy than metallic copper Cu (0) which can be observed in Figure.7. The XANES results for calcined catalysts are indicating the presence of Cu^{2+} in the bulk of CuO which is characterized by the edge position located at near 8990 eV, corresponding to the maximum of the first derivative (Figure.7 and S5). The XANES spectrum of CuO has displayed two characteristic features of Cu^{2+} ($3d^9$) compounds[42] with a pre-edge absorption at 8979 eV, and shoulder at 8986 eV that determines 1s→4p 'shake-down' transition in copper. Cu-Co/SiO_2 (X/Y=1) has resemblance to the CuO characteristic XANES spectrum indicating the presence of Cu^{2+}. However, relative to crystalline CuO, the calcined Cu-Co (X/Y=1) supported on H-ZSM-5, γ-Al_2O_3, and Cu-Co/γ-Al_2O_3 (X/Y=1, 2, 4) have an additional deep white line (first peak after the absorption edge), indicating higher 4pσ density of state.[43] The EXAFS Fourier transform modulus for fresh Cu-Co (X/Y=1) calcined catalysts over various supports and Cu-Co/ γ-Al_2O_3 (X/Y=1, 2, 4) are displayed in Figure.S6.

ARTICLE   **RSC Advances**
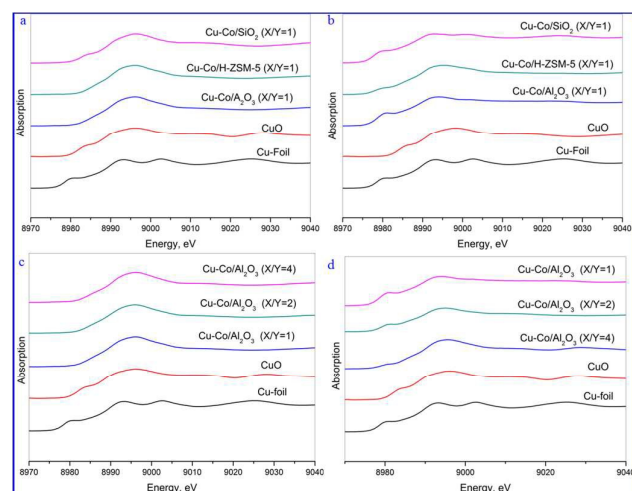
Figure.7 X-ray absorption near spectroscopy (XANES) spectra of Cu-Co(X/Y=1) over various supports (a) Fresh calcined 450 ^{o}C, (b) Reduced at 280 ^{o}C, and Cu-Co/γ-Al$_2$O$_3$ with various Cu/Co ratios (X/Y= 1, 2, and 4) (c) Fresh calcined 450 ^{o}C, (d) Reduced at 280 ^{o}C

Cu-Co (X/Y=1) supported on H-ZSM-5, and γ-Al$_2$O$_3$ displayed a peak in EXAFS Fourier transform modulus at 4.90 Å (refer. Figure S6) indicating the presence of mixed oxide CuCo$_2$O$_4$ which can be attributed to the distance between Cu^{2+}- Co^{3+} in the mixed oxide[33]. However, related peak was almost absent in the Cu-Co/SiO$_2$ (X/Y=1) catalyst which almost resembles the CuO Fourier transform modulus. These results validate those obtained by XRD analysis. The XANES and derivative XANES results of reduced catalysts indicate the presence of metallic Cu, and have the similar absorption energy pattern as that of the copper edge of copper foil (8979 eV). The quantity of CuO, and Cu (0) can be estimated from the XANES spectrum by Linear Combination Fitting in the Athena program.[44,45] Cu foil and CuO is used as a reference material to fit the data of reduced catalysts samples. The LCF results are summarized in the Table.2. As expected, the reduction of CuO to Cu metal is more in Cu-Co/γ-Al$_2$O$_3$ (X/Y=1) instead of Cu-Co/SiO$_2$ and Cu-Co/H-ZSM-5 (X/Y=1) catalysts. This is due to preferential localization of Cu particles in the uniform porous alumina. Furthermore, incorporation of cobalt metal improved the reducibility of Cu-Co/γ-Al$_2$O$_3$ catalysts, thus improving the catalytic activity. Nevertheless, we have studied Co-K edge XANES of fresh and reduced Cu-Co/γ-Al$_2$O$_3$ (X/Y=1) so as to determine the reduction of Co$_3$O$_4$ (Figure. S7). The fresh catalyst showed similar spectra which is characterized by Co$_3$O$_4$ spectrum. However, XANES spectra of reduced Cu-Co/γ-Al$_2$O$_3$ (X/Y=1) was slightly shifted towards lower energy level, and its pre-edge appeared probably in between Co-foil and Co$_3$O$_4$. Thereby, Co-K edge, XANES spectra indicate the presence of Co$_3$O$_4$ in fresh calcined catalysts and the partial reduction of Co$_3$O$_4$ to CoO in reduced catalyst.

Table 2. Cu-K edge LCF data of reduced catalysts

Catalysts	X/Y	% CuO	%Cu(0)
Cu-Co/SiO$_2$	1	54	46
Cu-Co/H-ZSM-5	1	35	65
Cu-Co/ γ-Al$_2$O$_3$	1	21	79
Cu-Co/ γ-Al$_2$O$_3$	2	38	62
Cu-Co/ γ-Al$_2$O$_3$	4	48	52

Catalytic activity

Effect of support on the catalytic activity
In order to investigate the effect of support, Cu-Co (x/y=1) catalysts supported on SiO$_2$, H-ZSM-5, and γ-Al$_2$O$_3$ were examined for the liquid phase hydrogenation of furfural to 2-MF at 200 ^{o}C, and 4.0 MPa (Figure 8). The results revealed 84% conversion of furfural over Cu-Co/SiO$_2$, and almost 99% conversion over Cu-Co/ γ-Al$_2$O$_3$ and Cu-Co/ H-ZSM-5 catalysts respectively. As expected, Cu-Co/SiO$_2$ (x/y=1) catalyst showed lower activity than other two catalysts (i.e., Cu-Co/γ-Al$_2$O$_3$, and Cu-Co/H-ZSM-5). Notably, weak metal-support interactions facilitate the dispersion of Cu, and thus the hydrogenation of furfural which was well supported by XRD, TEM, XANES, and H$_2$-TPR results. However, the selectivity towards 2-MF to a greater extent depends on the type of support, Co loading and/or both. For eg., minimum 2-MF and/or maximal FOL selectivity was obtained over Cu-Co/SiO$_2$ due to the presence of large Cu particles. The highest selectivity towards 2-MF was obtained over Cu-Co/γ-Al$_2$O$_3$ due to the presence of an additional number of Cu-CoOx which seems to be a key reason for enhanced MF formation, wherein, both the metallic copper and partially reduced CoOx have acted as active sites, favouring the conversion of intermediate FOL to 2-MF. As reported, Cu preferentially reduced the C=O bond but the reduction of C-O was difficult over Cu catalysts. Xu et al.[34] have reported that CoOx can effectively break the C-O bond and lead to a high selectivity to pentanediol from furfural. Hence, it is proposed that the combination of CuO and CuCo$_2$O$_4$ effectively break the C-O bond of intermediate FOL during reaction via –CH$_2$-OH hydrogenolysis which resulted in selective production of MF.[35]
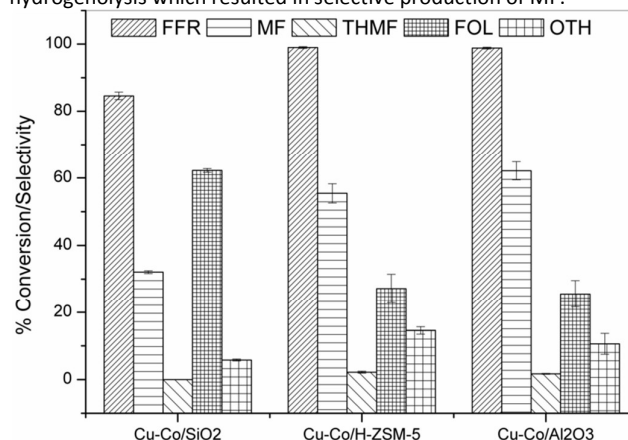
Figure 8. Catalytic activity of bi-metallic Cu-Co (x/y=1) over different supports for hydrogenation of furfural

(Reaction Conditions: T= 200°C, P= 4.0 MPa, furfural concentration = 2.25 M, Time = 4 h)

Furthermore, even though bi-metallic catalysts (Cu-Co/γ-Al$_2$O$_3$, and Cu-Co/H-ZSM-5) have resemblance in their catalytic structures as evident from XRD and XANES/EXAFS, Cu-Co/γ-Al$_2$O$_3$ is found to be more selective towards MF (Figure.8). The increasing number of mixed Cu-CoOx species in Cu-Co/γ-Al$_2$O$_3$, having ordered metal particles with uniform porosity which responsible for more selective production of MF. However, the combined results from XANES/EXAFS, TEM, and H$_2$-TPR studies revealed the presence of copper-cobalt nanoparticles with wide ranging shape and size and having comparatively less Cu-CoOx. In addition, these bi-metallic nanoparicles are un-evenly distributed on micro/meso porous H-ZSM-5. Thus, Cu-Co/H-ZSM-5 showed relatively less hydrogenolysis activity in comparison with Cu-Co/γ-Al$_2$O$_3$. The order of the

selectivity towards 2-MF for this reaction is as follows: Cu-Co/γ-Al$_2$O$_3$ > Cu-Co/H-ZSM-5> Cu-Co/SiO$_2$.

To further investigate the reaction pathways and address the enhanced hydrogenolysis activity, we examined the liquid phase hydrogenation of furfuryl alcohol over the same catalysts under same reaction conditions (Figure9). As expected, hydrogenolysis activity of Cu-Co/SiO$_2$ catalyst was much lower than the other two catalysts. Only 68% FOL got converted over Cu-Co/SiO$_2$ with 42% selectivity towards MF. Interestingly, THFOL was observed to be the next selective product over Cu-Co/SiO$_2$, which might be due to the saturation of the furan ring over metallic Cu. However, both Cu-Co/H-ZSM-5 and Cu-Co/γ-Al$_2$O$_3$ displayed slightly different trends than that observed with furfural hydrogenation. On comparative basis, Cu-Co/γ-Al$_2$O$_3$ exhibited higher hydrogenolysis activity (92% conversion of FOL) with 72% selectivity towards MF. In addition, the selectivity of pentanol (POL), derived from C2-O2 hydrogenolysis of 2-methylfuran[46], also increased significantly over Cu-Co/ γ-Al$_2$O$_3$. Cu-Co/H-ZSM-5 showed 84% conversion of FOL with 52% selectivity towards MF. Notably, Cu-Co/H-ZSM-5 produced higher amount of THMF and THFOL and other hydrogenated products than Cu-Co/γ-Al$_2$O$_3$. These findings strengthen the results obtained in the case of one-step hydrogenation of furfural to MF.
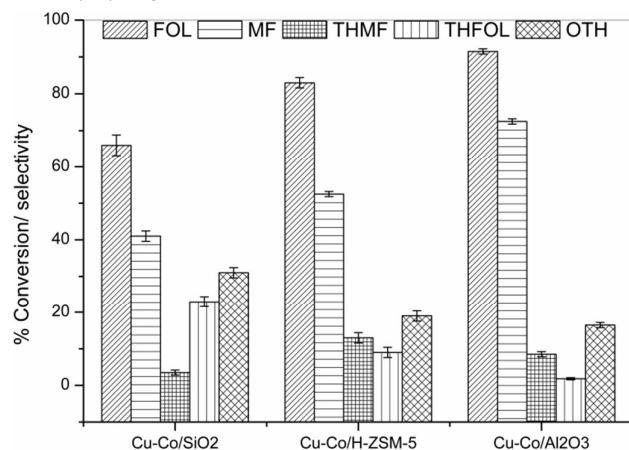
Figure 9. Catalytic activity of bi-metallic Cu-Co (x/y=1) over different supports for hydrogenation of furfuryl alcohol

(Reaction Conditions: T= 200°C, P= 4.0 MPa, FOL concentration = 2.25 M, Time = 4 h)

Effect of Cu/Co molar ratio(x/y) on the catalytic activity

In order to depict the role of Cu/Co ratio on the catalytic activity in the liquid-phase hydrogenation of furfural, bi-metallic Cu-Co/γ-Al$_2$O$_3$ with (x/y=1, 2, and 4) were examined at 200 ^{o}C and 4.0 MPa. The results were compared with monometallic Cu/γ-Al$_2$O$_3$ (10 wt %) (Table.3). As observed, Cu/γ-Al$_2$O$_3$ (10 wt %) displayed low conversion of furfural of nearly 92.6%, with moderate selectivity of 2-MF (44%). In contrast, by introducing cobalt as a co-metal, the activity of the resulting bi-metallic catalysts was increased (Table 3). The hydrogenation on monometallic Cu/γ-Al$_2$O$_3$ is expected to be less due to the much lower affinity of the surface for H$_2$ dissociation. Increase in the activity of bi-metallic Co-Cu catalysts may be attributed to a hydrogen spill-over effect whereby the aldehyde hydrogenation reaction takes place. Incorporation of Co as a co-metal helps to form mixed Cu-Co oxides due to strong interaction between Cu and Co as evident from XRD and XANES analyses. Thereby, H$_2$ consumption by both CuO and CoOx may have contributed proportionately to their available weight

proportion to the reduction process as a result of spill-over effects, thus improving the activity of bi-metallic system.[47] Furthermore, the selectivity of 2-MF increased with a decrease in the Cu/Co ratio (x/y= 4 to 1), and Cu-Co/ γ-Al$_2$O$_3$ (x/y=1) displayed the highest selectivity towards 2-MF (62%). However, the effect of Cu/Co ratio was insignificant for the conversion of FFR. The increased selectivity of 2-MF can be attributed to the increase in the number of CoOx phases, copper metal, and weak acid sites, as Cu-Co/Al$_2$O$_3$ (X/Y=1) shows the maximum number of Co$_3$O$_4$/CuCo$_2$O$_4$ phases, copper metal, and the weak acidity (refer Figure. S1 & Table.S3) which are accountable for the increased rate of hydrogenolysis, and the resultant maximum selectivity of MF.[34,48]

Table.3 Effect of Cu/Co (x/y) on the catalytic activity of bi-metallic Cu-Co catalysts supported on γ-Al$_2$O$_3$

Catalysts	Loading		% X_{FFR}	%S			
	x/y	Cu (wt%)		2-MF	THMF	FOL	O_{TH}
Cu/ γ-Al$_2$O$_3$		10	92.6	44.6	0.2	46.4	8.8
Cu-Co/ γ-Al$_2$O$_3$	1	10	98.8	62.1	1.7	25.6	10.6
Cu-Co / γ-Al$_2$O$_3$	2	10	99.0	58.4	1.2	22.2	18.2
Cu-Co / γ-Al$_2$O$_3$	4	10	99.0	54.2	0.8	20.8	24.2

(Reaction Conditions: T= 200 ^{o}C, P= 4.0 MPa, furfural concentration = 2.25 M, Time = 4 h)

Effect of temperature on the activity of Cu-Co/γ-Al$_2$O$_3$ (x/y=1)

Control of the reaction temperature on the catalytic activity for Cu-Co/γ-Al$_2$O$_3$ (x/y=1) is shown in Figure 10. It is interesting to see that the reaction temperature plays an important role in the product distribution. It was observed that FOL is the main product at low temperature (140 °C), and selectivity towards 2-MF increased with an increase in reaction temperature from 140 to 220 $^\circ$C. The furfural conversion increased from 94.6% (140 °C) to 100 % (220 °C).
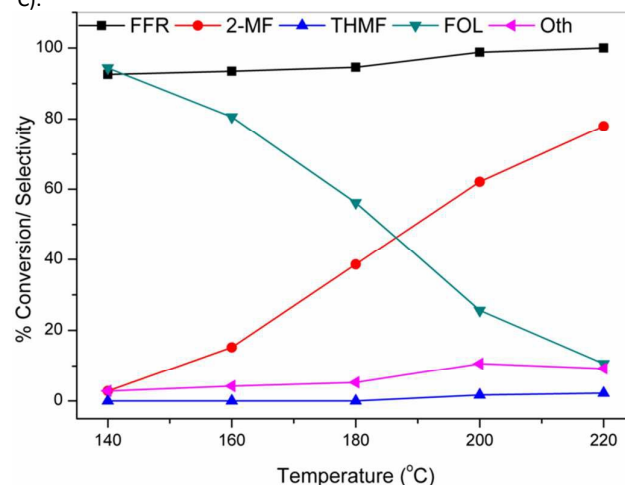
Figure .10 Effect of temperature on the selectivity of 2-MF over Cu-Co/γ-Al$_2$O$_3$(x/y=1) via Furfural hydrogenation

(Reaction Conditions: P= 4.0 MPa, furfural concentration = 2.25 M, Time = 4 h)

ARTICLE   RSC Advances
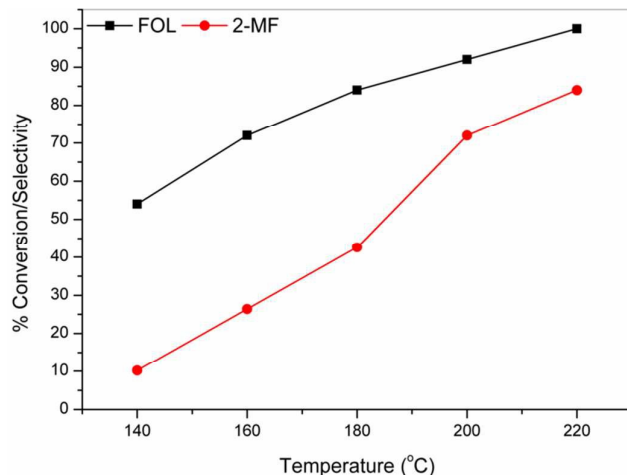
Figure .11 Effect of temperature on the selectivity of 2-MF over Cu-Co/ɣ-Al$_2$O$_3$(x/y=1) via FOL hydrogenolysis

(Reaction Conditions: P= 4.0 MPa, FOL concentration = 2.25 M, Time = 4 h)

The selectivity of desired 2-MF was found to be 78 % with 100 % conversion of furfural. The selectivity of 2-MF at a lower temperature (<200 °C) was very low, due to the presence of intermediate furfuryl alcohol. It is worth noting that higher temperature promotes the C-O hydrogenolysis for the cleavage of the carbonyl group due to the higher activation of the C-O bond [19]. Therefore, the rise of temperature is much more important for the -CH$_2$-OH hydrogenolysis of the intermediate FOL. However, beyond certain temperature, further increase in temperature will increase the rate of hydrogenolysis and form other hydrogenolysis products such as 2-pentanone, 1-pentanol, and 2-pentanol. In order to examine the conversion of intermediate FOL to 2-MF, the effect of temperature was also studied for hydrogenation of furfuryl alcohol (FOL) to 2-MF over the temperature range from 140 to 220 °C. The results revealed the similar trend for the selectivity towards 2-MF as observed with FFR hydrogenation. The selectivity of 2-MF was increased with increasing temperature and reached the maximum of 84 % (Figure.11). These observations suggest that hydrogenation of FFR to FOL is a metal catalyzed reaction which favours at lower temperature whereas, hydrogenolysis of FOL to 2-MF occurs at a high temperature which is be catalyzed by mixed copper-cobalt species.

Catalysts reusability for liquid phase hydrogenation of furfural

Cu-Co/ɣ-Al$_2$O$_3$(x/y=1) catalyst that exhibited the best catalytic efficiency was recycled three times to evaluate its stability. Owing to possible deposits (organic reactant/products and/or possible carbon deposits) on the catalyst surface during the catalytic reactions, catalyst was dried in an inert atmosphere at 100 °C followed by calcinations at 500 °C to remove potentially adsorbed or deposited organic/carbon species. The used catalyst without calcinations (2nd Cycle, dried at 100°C) is characterized using TEM, XRD, and CHNS analysis to determine the possible deposits of organic template and/or carbon on the active sites (refer.Figure.3d, S2, and Table. S4). The XRD pattern of used catalyst resembles the characteristic features of ɣ-Al$_2$O$_3$. Furthermore, as compared with Cu-Co/ɣ-Al$_2$O$_3$(x/y=1) catalyst, no peak corresponding to Cu, Co, and/or their mixed phases were observed (Figure. S2). This can be attributed to the possible deposition of carbon over active sites. However, the absence of carbon peaks in XRD pattern indicates the

uniform distribution of carbon. The XRD result of used catalyst is well supported by TEM and CHNS analyses, which have confirmed the presence of carbon (Figure.3d, Table. S4). Furthermore, TEM results demonstrate that not only carbon deposited on the active sites but also the size of particles slightly increased after 2nd cycle which may be the reason for a drop in the activity of catalysts In order to explore the recyclability of Cu-Co/Al$_2$O$_3$(X/Y=1) catalysts, the used catalyst was separated from a reaction mixture and dried at 100 °C for overnight in the oven. The hydrogenation of furfural was then performed over the used catalyst with and without calcination (Table.4).

Table.4 Reusability of Cu-Co/ɣ-Al$_2$O$_3$(x/y=1) catalyst toward hydrogenation of furfural to 2-methylfuran

Catalysts	X$_{FFR}$ (%)	S$_{2-MF}$(%)
Cu-Co/ɣ-Al$_2$O$_3$(x/y=1) Fresh	100	78.0
^{a}Cu-Co/ɣ-Al$_2$O$_3$(x/y=1) 1st cycle	88.6	59.5
^{a}Cu-Co/ɣ-Al2O3(x/y=1)2nd cycle	72.2	40.6
^{b}Cu-Co/ɣ-Al$_2$O$_3$(x/y=1) 1st cycle	99.2	77.2
^{b}Cu-Co/ɣ-Al$_2$O$_3$(x/y=1) 2nd cycle	94.2	76.8
^{b}Cu-Co/ɣ-Al$_2$O$_3$(x/y=1) 3rd cycle	93.6	76.4

(X$_{FFR}$ = conversion of furfural, S$_{2-MF}$ = Selectivity of 2-methylfuran)
(Reaction Conditions: T= 220 °C, P= 4.0 MPa, furfural concentration = 2.25 M, Time = 4 h)
^{a}no calcination
^{b}calcination

A significant decrease in conversion of furfural was observed after the catalyst was reused twice (from 100 to 72%) without calcinations. However, a slight decrease in the conversion of FFR (nearly 7 % up to 3rd cycle) was observed over calcined catalysts owing to re-dispersion of active sites by coke burn off during calcinations. Thus, it could be concluded that catalyst had lost its activity due to coke formation during the hydrogenation of furfural, covering active sites of catalysts.

Conclusion

Three supported bi-metallic catalysts (Cu-Co/SiO$_2$, Cu-Co/ɣ-Al$_2$O$_3$, and Cu-Co/H-ZSM-5) with various Cu/Co molar ratios (x/y) were prepared and examined for the one-step liquid phase hydrogenation of furfural to 2-MF. The inherent properties of carriers, and the strong interaction between Cu and Co have significant influence on the catalytic performance of bi-metallic Cu-Co catalysts towards the production of 2-MF. Cu-Co catalysts supported over acidic carrier are found to be much more selective towards MF owing to the formation of spinel CuCo$_2$O$_4$ oxides, and much higher dispersion of Cu on acidic supports such as H-ZSM-5, and ɣ-Al$_2$O$_3$. On the other hand, Cu-Co/SiO$_2$ found to be less active and selective towards MF due to the presence of large Cu particles. Amongst three catalysts, Cu-Co/ ɣ-Al$_2$O$_3$ (x/y=1) exhibited the best catalytic performance. The conversion of furfural and the selectivity towards 2-MF were as high as 100% and 78%, respectively, at 220 °C and 4.0 MPa. Systematic characterization techniques revealed that Cu-Co/ɣ-Al$_2$O$_3$ (x/y=1) catalyst had more Cu-CoOx phases which are accountable for hydrogenation/hydrogenolysis of furfural to MF. Moreover, present study explored the role of support acidity and metal-support interactions, which greatly influences particle size distribution/dispersion and reducibility of active sites, which in turn provided in depth insight for the rational design of a robust bi-metallic catalyst system for the hydrogenation and/or hydrogenolysis reactions. Further studies are being focused on optimization of process parameters, kinetics and mechanism of this

reaction so as to provide basis for the reactor design and scale up studies.

References

1   D. M. Alonso, S. G. Wettstein and J. A. Dumesic, Chem. Soc. Rev., 2012, 41, 8075-8098.
2   S. Datta, S. De, B. Saha and I. Alam, Catal. Sci. Tech., 2012, 2, 2025–2036.
3   P. Gallezot, Chem. Soc. Rev., 2012, 41, 1538-1558.
4   J. A. Melero, J. Iglesias and A. Garcia, Ener. Env. Sci., 2012, 5, 7393-7420.
5   Corma, S. Iborra and A. Velty, Chem. Rev., 2007, 107, 2411–2502.
6   Y Elkasabi, C. A. Mullen, L. M. T. Pighinelli and A. A. Boateng, Fuel Processing Tech. 2014, 123: 11-18.
7   M. Wei, B. Haoxi and A. Ragauskas, BioEnergy Research, 2013, 6, 1183-1204.
8   W. Yang and A. Sen, Chem. Sus. Chem. 2011, 4, 349-352.
9   B. Danon, G. Marcotullio and W. D. Jong, Green Chem., 2014, 16, 39-54.
10 K. Yan and A. Chen, Energy 2013, 58, 353-363.
11 K. Yan and A. Chen, Fuel 2014, 115, 101-108.
12 K. Yan, L. Jiayou, X. Wu and X. Xianmei, RSC Advances, 2013, 3, 3853.
13 P. Panagiotopoulou, and D. G. Vlachos, Appl. Catal. A: Gen.., 2014, 480, 17-27.
14 L. D. Plyusnin, T. V. Beisekov, M. S. Erzhanova and B. D. Daurenbekov, Khim.Prom-st. 1988, 11, 672.
15 M. M Villaverde, N. M. Bertero, T. F. Garetto and A. J. Marchi, Catal. Today 2013, 213, 87-92.
16 D. V. Hernandez, J. M. Rubio-Caballero, J. Santamarıa-Gonzalez, R. Moreno-Tost, J. M. Merida-Robles, M. A. Perez-Cruz, A. Jimenez-Lopez, R. Hernandez-Huesca and P.Maireles-Torres, J. Mol. Catal. A: Chem., 2014, 383-384, 106-113.
17 B. M. Nagaraja, A. H. Padmasri, B. D. Raju and K. S. RamaRao, J. Mol. Catal. A. Chem. 2007, 265, 90-97.
18 H. Y. Zeng, Y. L. Zhu, L. Huang, L., Z. Y. Zeng, H. J. Wan and L. W. Li, Catal. Comm., 2008, 9, 342–348.
19 S. Sitthisa, A. Wei and D. E. Resasco, J. of Catal. 2011, 284, 90–101.
20 P. Panagiotopoulou, N. Martin and D. G. Vlachos, J. of Mol. Catal. A: Chem., 2014, 392, 223-228.
21 M. Hronec and K. Fulajtarová, Catal. Comm., 2012, 24, 100–104.
22 S. Gowada, S. Parkin and F. T. Ladipo, AOC, 2012, 26, 86-93.
23 J. Y. Lee, D. W. Lee, K. Y. Lee and Y. Wang,   Catal. Today, 2009, 146, 260-264.
24 Y. J. Fang, Y. Liu and L. H. Zhang, Appl. Catal. A: Gen., 2011, 397, 183-19.
25 S. Yin and Q. Ge, Catal. Today, 2012, 194, 30– 37.
26 B. M. Reddy, G. K. Reddy, K. N. Rao, A. Khan and I. Ganesh, J. of Mol. Catal. A. 2007, 265, 276-282.
27 S. Srivastava, N. Solanki, P. Mohanty, K. A. Shah, J. K. Parikh and A. K. Dalai, Catal. Lett., 2015, 145, 816-823.
28 S. Srivastava, P. Mohanty, J. K. Parikh, A. K. Dalai, S. S. Amritphale and A. K. Khare, Chin. J. of Catal. 2015, 36, 933-942.
29 G.R. Sheffer, R. A. Jacobson and T. S. King, J. Catal. 1989, 116, 95.
30 M. Blanchard, H. Derule and P. Canesson, Catal. Lett. 1989, 2, 319.
31 J.E. Baker, R. Burch, S.J. Hibble and P. K. Loader, Appl. Catal. 1990, 65, 281.
32 J.E. Baker, R. Burch and S.E. Golinski, Appl. Catal. 1989, 53, 279.
33 J. Wang, P. A. Chernavskii, A. Y. Khodakov and Y. Wang, J. Catal. 2012, 286, 51–61
34 W. Xu, H. Wang, X. Liu, J. Reu, Y. Wang and G. Lu, ChemComm, 2011, 47, 3924-3926.
35 P. A. Ramachandran and R. V. Chaudhari. Three-Phase Catalytic Reactors. New York: Gordon and Breach, 1983. 427
36 B. M. Nagaraja, V. S. Kumar, V. Shasikala, A. H. Padmasri, B. Sreedhar, D. V. Raju and K. S. Rama Rao, Catal. Comm., 2003, 4, 287–293.
37 J. Wang, P. A. Chernavskii, Y. Wang and A. Y. Khodakov, Fuel 2013, 103, 1111–1122.
38 G. C. Bond, Platinum Metals Review, 1983, 21, 16-18.
39 Y. Lai, M. N. Rutigliano, and G. Veser, Langmuir, 2015, 31, 10562−10572
40 D. V. Cesar, A. P. Carlos,. V. M. M. Salim and M. Schmal, Appl. Catal.A: Gen., 1999, 176,205-212.
41 A. J. Marchi, J. I. Cosimo and C. R. Apesteguia, Catal. Today, 1992, 15, 383-394.
42 I. J. Drake, K. L. Fujdala, S. Baxamusa, A. T. Bell and T. Don Tilley, J. Phys. Chem. B. 2004, 18421.
43 G. Silversmit, H. Poelman, V. Balcaen, P. M. Heynderickx, M. Olea, S. Nikitenko, W. Bras, P. F. Smet, D. Poelman, R. De Gryse, M. F. Reniers and G.B. Marin, J. Phys. Chem. Solids, 2009, 70, 1274.
44 B. Ravel and M. Newville, J. Synchrotron Rad. 2005, 12, 537.
45 K. An, N. Musselwhite, G. Kennedy, V. V. Pushkarev, L. R. Baker and G. A. Somorjai, J. of Coll. and Int. Sci., 2013, 392, 122–128.
46 J. Kijenski, P. Winiarek, T. Paryjczak, A. Lewicki and A. Mikolajska, Appl. Catal. A: Gen. 2002, 233, 171-182.
47 L. J. Malobela, J. Heveling, W. G. Augustyn and L. M. Cele, Ind. Eng. Chem. Res., 2014, 53, 13910–13919
48 M. J. Gikey, P. Panagiotopoulou, A. V. Mironenko, G. R. Jenness, D. G. Viachos, and B. Xu, ACS Catal. 2015, 7, 3988-3994.

RSC Advances Accepted Manuscript

Graphical Abstract
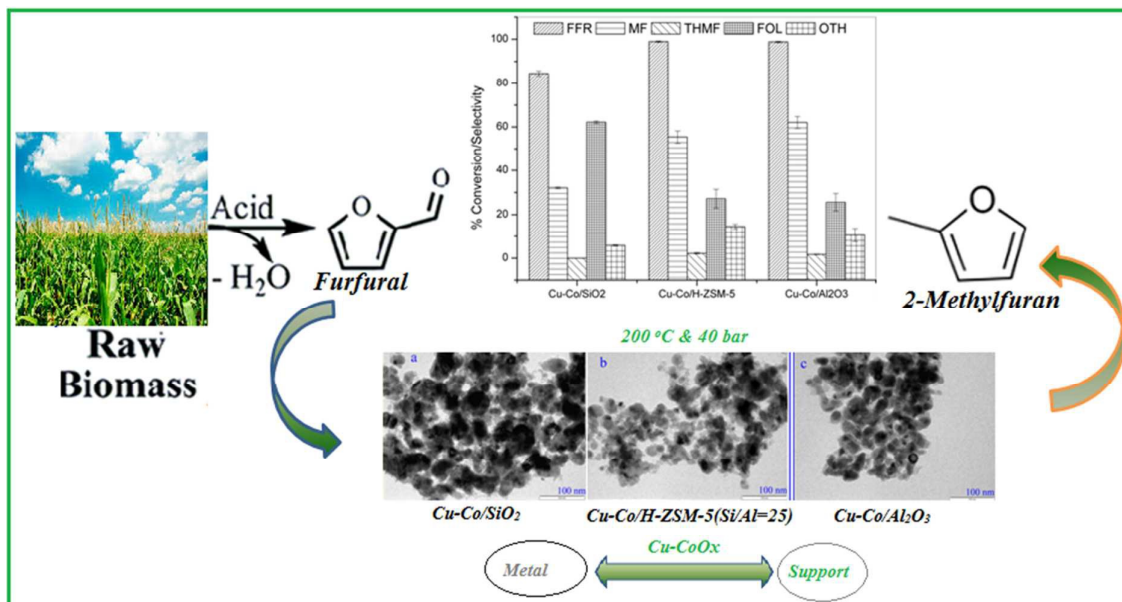
This work presents the application of bi-metallic copper-cobalt catalysts towards one step hydrogenation of furfural to 2-methylfuran in liquid phase.